VOL. 2, NO. 1, MARCH 2013 ISSN 2305-493X
ARPN Journal of Earth Sciences


www.arpnjournals.com

HIMALAYAN LAND COVERS CLASSIFICATION WITH ECOLOGICAL CONCERN USING EO-1 HYPERION

Manjeet Singh[1], V. D. Mishra[2], G. Saravana[2], Jyoti Dhar Sharma[1] and Anita Negi[3]
[1]Department of Physics, Shoolini University, Solan (H. P), India
[2]Snow and Avalanche Study Establishment, DRDO, Chandigarh (U.T), India
[3]Indian Institute of Ecology and Environment, New Delhi, India
E-Mail: thakur.m82@gmail.com

ABSTRACT

Land cover is the assemblage of biotic and abiotic components on the earth's surface and has direct concern with ecology. The sensitivity of the earth's climate as well as ecological system depends on land cover changes. This gives immense importance to study the land cover changes especially when satellite data provides timely and efficient information about large land area. In the present paper, the study was carried out by using NASA's hyperspectral EO-1 Hyperion sensor for middle and upper zone of Himalaya. The analysis procedure consists of Fast Line-of-sight Atmospheric Analysis of Spectral Hypercubes (FLAASH) atmospheric correction code derives its physics-based algorithm from the Moderate Resolution Transmittance (MODTRAN4) radiative transfer code as well as radiometric (atmospheric + topographic) correction to retrieve surface reflectance. Various statistical models for supervised classification such as spectral angle mapper (SAM), support vector machine (SVM), and maximum likelihood (MLH) has been examined and validated with existed Normalized Difference; Vegetation Index (NDVI), Snow Index (NDSI) and Glacier Index (NDGI) models. The spectral reflectance of different surface parameters has been collected in field, using spectro-radiometer and compared with satellite derived spectra. Presently land cover classification accuracy assessments are based on error matrix, which is a simple cross-tabulation of the mapped class against that observed in the reference data at a set of validation. Study distills these statistical approaches into a unique set of hierarchical taxonomy that reveals the similarities and differences between algorithms.

Keywords: land cover, hyperion, FLAASH, MODTRAN, SAM, MLH, SVM.

INTRODUCTION

Himalaya is one of the youngest folded mountainous formations of the world, characterized by a complex geologic structure, snowcapped peaks, large valley glaciers, deep river gorges and rich soil and vegetation. A complex interplay of climatic and geological processes led to resource degradation in Himalayan ecosystem (Jodha, 2001). Changes in ecosystems are generally affected by the level and type of land surface parameters such as land covers which includes: snow, water, grassland, forest, and bare soil (Assefa, 2004). And extraction of surface parameters has world-wide concern to understand its impact on radiation balance, local climate, global climate change, biogeochemistry, diversity and abundance of terrestrial species. Thus an accurate representation of surface parameters and biophysical attributes (soils, elevation, topography-slope and aspect, etc.) of the landscape within Himalaya is required (Manjeet *et al*., 2012). In the last three decades, considerable advancement in space technology providing a numerous satellite platforms to study complex physical processes of the earth-atmosphere system (Rogan and Chen, 2004). And one of the best basic characteristics of remote sensing is the extensive use of quantitative algorithms for estimating earth surface variables (Liang, 2004). The accurate estimation of surface variable using coarse resolution satellite sensor is challenging task due to mixing of various heterogeneous land features in a pixel. Sub-pixel classification techniques using multispectral data have been reported by many authors (Nolin *et al*., 1993; Rosenthal and Dozier, 1996; Simpson *et al*., 1998; Metsamaki *et al*., 2002; Vikhamar and Solberg, 2002; Haertel and Shimabukuro, 2005) to improve the accuracy of classification for many applications in the field of earth surveys. However, for certain applications there is a limit in the spatial and spectral resolution of satellite sensor which restricts the usefulness of multispectral data (Mishra *et al*., 2010). To get full advantages of spatial and spectral resolution, hyperspectral imagery EO-1 Hyperion provides opportunities to extract more detailed information than traditional multispectral data. The main objective of the present paper is to extract land surface parameters middle and upper ranges of Himalayas with varying altitude from 1100m to 6000m. Three key issues of the present work (a) potential of Hyperion data for land cover classification (b) estimation of land cover characteristics at sub pixel level (c) multi-temporal input to ecological modeling, has achieved by various statistical models of supervised classification such as spectral angle mapper (SAM), support vector machine (SVM), and maximum likelihood (MLH) and validate/compare with existed models. Overall accuracy of the model is accessed by regression analysis and root mean square error.

STUDY AREA

The study area is divided in two different zones of Himalaya. 1st study area is located in Greater Himalayan Zone that lies between $32^0$11'40''N to $32^0$17'46'' N latitude and $78^0$30'13''E to $78^0$30'14''E longitude, also known as middle Himalaya (Negi *et al*.,

2010) which is characterized by fairly cold temperatures, heavy snowfall and higher elevations and the 2nd study area is located in the Karakoram Range of upper Himalayan Zone lies between $35^0$42'7''N to $35^0$48'13''N and $76^0$20'5''E to $76^0$20'6''E. The majority of the slopes inclination lies in the range of 55-60 degree. Figure-1 show different Himalayan ranges in study area on SoI map and on different satellite images.

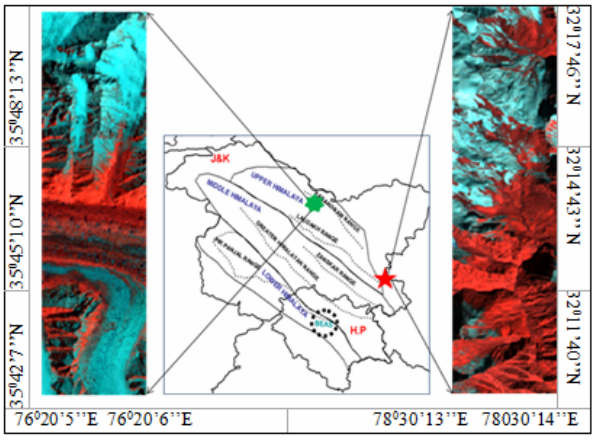

Figure-1. Study area on India map with different ranges of Himalaya and Hyperion satellite images of middle and upper Himalayan zone.

Satellite data and sensor description

The study was carried out with Level 1_A: L1G/L1T data (geometric and terrain corrected) of Hyperion sensor onboard NASA's Earth Observing one (EO -1) platform. Hyperion collects 220 unique spectral channels ranging from 357nm to 2576nm with a 10-nm bandwidth (USGS user guide, 2003). The instrument operates in a push broom fashion, with a spatial resolution of 30 meters for all bands with a standard scene width of 7.7 kilometers. The data is available in 16-bit signed integer's radiance values.

METHODOLOGY

Satellite data processing

Hyperion sensor covered the wavelength region by two detector arrays, one for the visible and near - infrared (VNIR: 356 nm to 1058 nm) and other for short-wave infrared (SWIR: 852 nm to 2577 nm) with 242 bands of 10 nm spectral resolution and 30 m spatial resolution (USGS user guide, 2003). But due to radiometric detraction and signal to noise issues only 198 bands are calibrated (Pearlman *et al*., 2003). The detail description of radiometric errors in Hyperion data are reported by (Datt *et al*., 2003, Bindschadler *et al*., 2003). As a result, only a subset of 158 bands maintained for further analysis. Hyperion satellite data was pre-processed in ENVI 4.7 software (ENVI User's Guide, 2009). The flow chart of the detailed methodology is given in Figure-2.

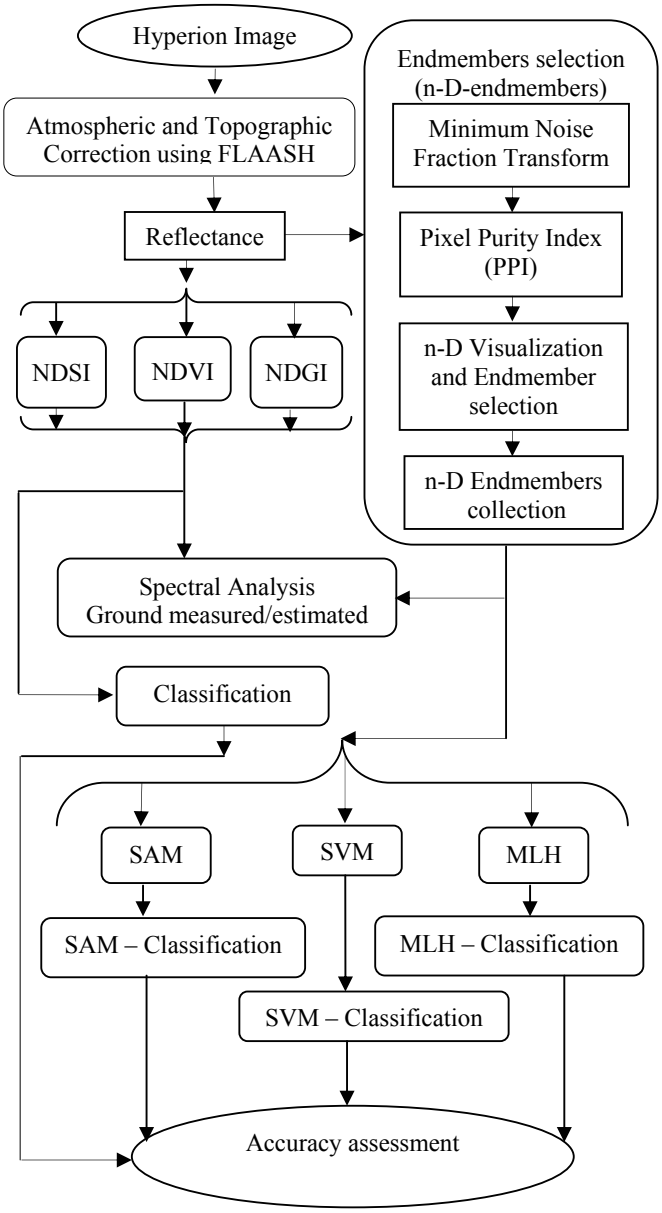

Figure- 2. Flow chart summarizing the methodology followed in the study

Radio metrically corrected reflectance

Atmospheric effects caused by molecular, particulate scattering and absorption from the 'radiance-at-detector has been eliminated by using Fast Line-of-sight Atmospheric Analysis of Spectral Hypercubes (FLAASH) module based on the MODTRAN-4 radiative transfer code (Anderson *et al*., 1999; Cooley *et al*., 2002) in order to retrieve 'reflectance-at-surface' values. FLAASH allows a researcher to define all parameters that influence atmospheric absorption and scattering such as relative solar position, aerosol and scattering models, visibility parameters, ozone total vertical column, adjacency effects (scattering of reflected radiance from surroundings into a pixel), artifact suppression (Matthew *et al*., 2000) and provides water vapor retrieval. In the present study,

atmospheric model with 2-band KT aerosol model (Kaufman *et al*., 1997) was used for atmospheric correction.

Digital values in Hyperion data represent absolute radiance ($W/m^2*\mu m*sr$) values stored as 16-bit signed integers with a scaling factor of 40 for VNIR bands and 80 for SWIR bands. The spectral radiance at sensor pixel using FLAASH is derived from a standard equation (Cooley *et al*., 2002) as:

$$L = Lgi + Lpi$$

$$Lgi = A\frac{\rho}{1-\rho iS} \quad \text{And}$$

$$Lpi = B\frac{\rho i}{1-\rho iS} + La$$

Where Lgi is the at-sensor radiance reflected by the target and Lpi is the at-sensor radiance scattered into the path by the atmosphere and the surrounding targets, (ρ) is the pixel surface reflectance, (ρ_i) is an average surface reflectance for the pixel and a surrounding region, (S) is the spherical albedo of the atmosphere and (La) is the radiance back scattered by the atmosphere. The coefficient A and B depends on atmospheric and geometric conditions but not on the surface. Each of these variables depends on spectral channels; the wavelength index has been omitted for simplicity.

The values of A, B, S and La are determined from MODTRAN4 calculations that use the viewing and solar angles and the mean surface elevation of the measurement, and they assume a certain model atmosphere, aerosol type, and visible range.

Surface parameters extraction

Hall *et at*., 1995 proposed Normalized Difference Snow Index (NDSI) method to identifying snow cover area and defined as:

$$NDSI = \frac{(\text{Green Reflectance} - \text{SWIR Reflectance})}{(\text{Green Reflectance} + \text{SWIR Reflectance})}$$

The reflectance of snow is high in the visible band and low in the SWIR band (Figure-3). The specific threshold value of NDSI of 0.4 is defined to allow identification of snow covered areas from images produced by different sensors (Hall *et al*., 1995; Xiao *et al*., 2001; Kulkarni *et al*., 2006). The identification of snow covered areas using conditional combination of NDSI and NIR band reflectance (NDSI>=0.4 and NIR >10%) therefore may not be accurate for the snow covered areas mixed with vegetation. Therefore it is necessary to change the threshold value of NDSI by considering to the Normal Difference Vegetation index (NDVI) for estimation of snow cover area under vegetation. The NDVI is estimated using the following equation:

$$NDVI = \frac{(\text{NIR Reflectance} - \text{Red Reflectance})}{(\text{NIR Reflectance} + \text{Red Reflectance})}$$

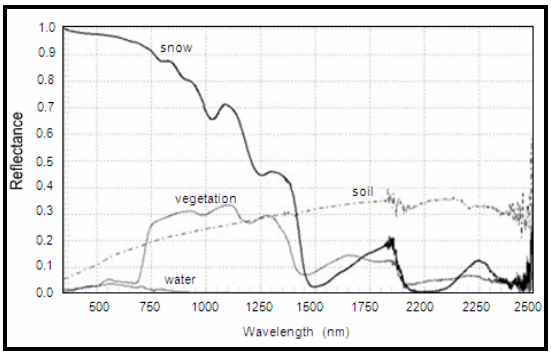

(a)

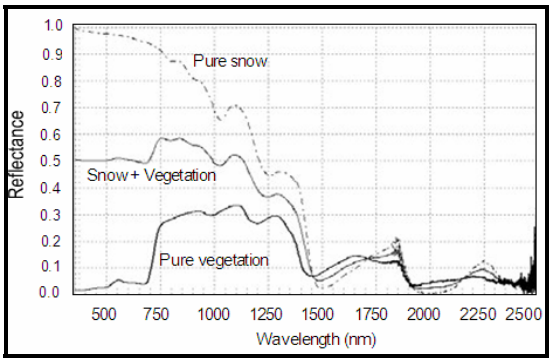

(b)

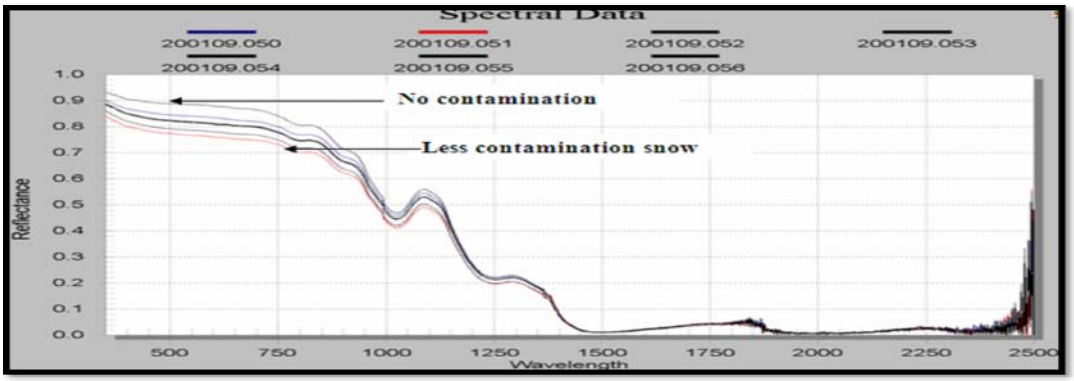

(c)

Figure-3. An in-situ measure spectral reflectance characteristic of different land covers (a) pure snow, soil, vegetation, water (b) Snow mixed vegetation (c) less contaminated snow/snow-ice mixed debris.

The methodology proposed by (Klein *et al*., 1998; Shimamura *et al*., 2006) has been adopted to define the threshold value of NDSI for snow cover monitoring under vegetation. Further discrimination within 'Snow + ice + ice-mixed debris (IMD)' proposed by A.K Keshri *et al*., 2009 in Normalized Difference Glacier Index (NDGI) as:

$$NDGI = \frac{(\text{Green Reflectance} - \text{Red Reflectance})}{(\text{Green Reflectance} + \text{Red Reflectance})}$$

The specific threshold value 0.025 has been chosen for the study area data set.

Land cover classification

Spectral angle mapper (SAM)

A physically-based classification spectral angle mapper (SAM) method was used in present study for the land-surface parameter extraction. The algorithm determines the spectral similarity between the two spectra (i.e., the pixel spectra to known/reference spectra) by calculating the angle between two vectors representing these spectra (Kruse *et al*., 2003).

Maximum likelihood (MLH)

Maximum likelihood classification assumes that the statistics for each class in each band are normally distributed and calculates the probability that a given pixel belongs to a specific class. Each pixel is assigned to the class that has the highest probability (that is, the maximum likelihood). ENVI implements maximum likelihood classification by calculating the discriminant functions for each pixel in the image (Richards *et al*., 1999).

Support vector machine (SVM)

To perform supervised classification on images, support vector machine (SVM) is used to identify the class associated with each pixel. It separates the classes with a decision surface that maximizes the margin between the classes. Present classification was done with SVM radial basis function (RBF) kernel. This kernel nonlinearly maps samples into a higher dimensional space so it can handle the case when the relation between class labels and attributes is nonlinear. The mathematical representation of radial basis function (RBF) kernel is listed below (Hsu *et al*., 2007):

$$K(x_i, x_j) = \exp(-\gamma \|x_i - x_j\|^2), \gamma > 0$$

Where γ is the gamma term in the kernel function for all kernel types except linear.

To evaluate all above selected methodology and classification results, the selection of endmembers based on "Spectral Hourglass" processing scheme (Kruse *et al*., 2003) were implemented. This Procedure includes the generation of Minimum Noise Fraction-Images (MNF) for data dimensionality estimation and reduction by decorrelating the useful information and separating noise (Green *et al*., 1988), Pixel Purity Index-Mapping (PPI) for the determination of the purest pixels in an image (as potential endmembers) utilizing the (uncorrelated) MNF-images and finally the extraction of endmembers utilizing the n-Dimensional-Visualizer tool (Figure-4).

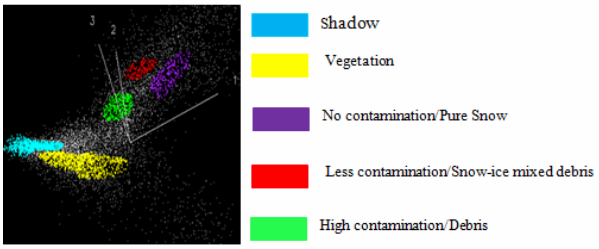

Figure-4. 3-D visualization for endmembers selection of different classes in Hyperion data (4-Dec-2011).

The extracted end member's spectra are then compared with the in-situ measured spectral reflectance using optical spectro-radiometer (Figure-3). The selected image spectra end members were further used as reference spectra for various surface parameters using SAM, MLH and SVM method. The threshold value of SAM angle for classification was set after iteration for tuning the angle between the pixel spectra and the reference spectra to avoid misclassification especially in the shadow regions.

RESULTS

Spectral analysis

In-situ observations of spectral reflectance using optical spectro-radiometer on the same day at the time of satellite pass are collected at number of points for pure snow, soil, vegetation, water, less contaminated snow (vegetation/soil mixed snow) samples (Figure-3). Due to inaccessible region at middle and upper Himalaya and non-availability of any image data with spatial resolution higher than 15m, Hyperion visible/near-infrared image was itself used as reference data. The test sample constituting 50 pixels per class was collected and reference class values to each point were given on the basis of analysis of spectral curves (Figure-5) which were compared with in-situ measured spectral reflectance (Figure-3) at field observatory (Lat/Log: $32^0$21'33''N/$77^0$7'43''E).

Retrieval of land surface parameters

A sequential classification of Himalayan land surface parameters such as pure snow/no contamination, less contaminated snow/snow-ice mixed debris, debris, soil and vegetation has retrieved with various statistical models (Figure-6). The comparative visual analysis of Hyperion for different dates obtained using SAM, SVM

and MLH is shown in Figure-6 ((c-d), (e-f) and (g-h)) respectively. In order to confirm the actual land cover area after atmospheric and topographic correction, the results are compared with existed methods (Figure-6 (a-b)) estimated Hyperion sensor. Mostly the shady areas in both ranges of Himalayas are unclassified with SAM technique. On the other hand MLH technique over classifying the surface parameters, whereas the appearance of different land covers using SVM (Figure-6 (e-f)) are quite similar with existed models (Figure-6 (a-b)). Figure-6 shows the thematic results of various land cover parameters.

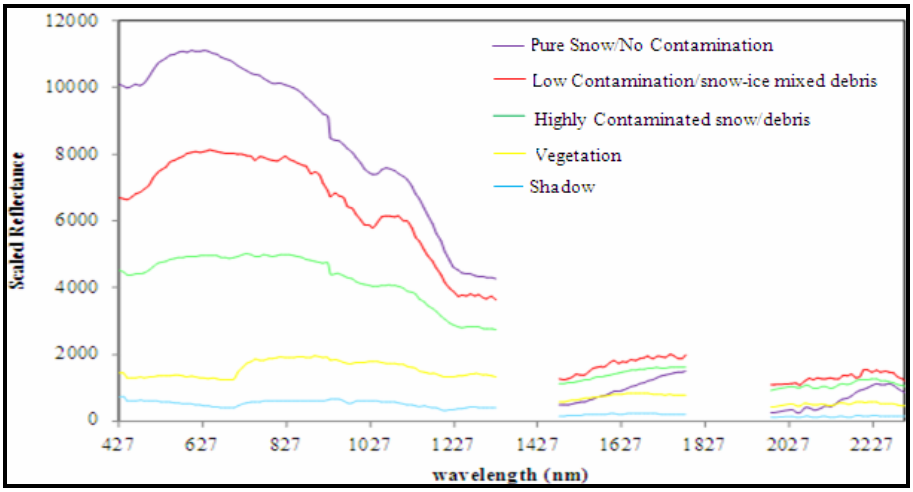

Figure-5. Hyperion (4-Dec-2011) spectral reflectance of land covers.

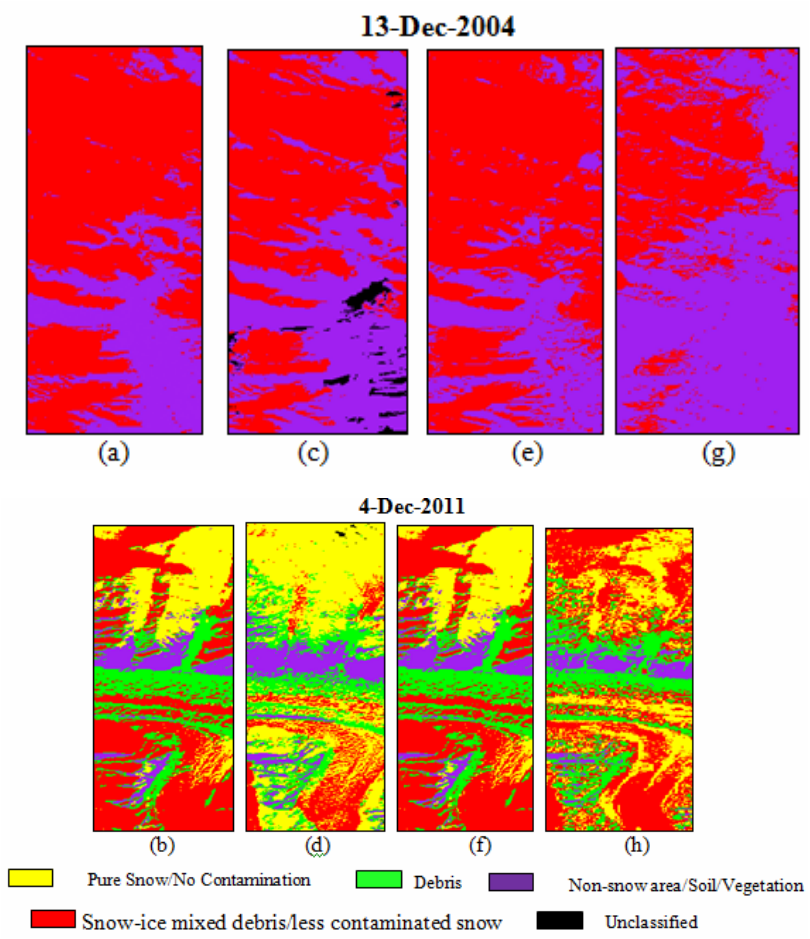

Figure-6. Thematic maps of land surface parameters using (a-b) existed models, (c-d) SAM, (e-f) SVM and (g-h) MLH on 13-Dec-2004 and 4-Dec-2011, respectively.

Statistical analysis and validation

For the purpose of validation the classified output, a statistical matrix-based approach is developed between existed and proposed models (Table-1). Regression analysis (Figure-7) of Hyperion data (4-Dec-2011) as well as tabular matrix approach (Table-1) supporting the strength of SVM as an additional tool to retrieve land surface parameters at lower, middle and upper Himalaya. Classification is not complete unless error analysis has been performed. In this paper, the root mean square error (RMSE) is calculated as follows (Salomon son and Appel, 2004)

$$RMSE = \sum_{i=1}^{M} \sqrt{\frac{1}{M}\sum_{j=1}^{n}\left(\frac{e_c^2}{n^2}\right)}$$

Where M is the number of bands and n is the number of pixels. RMSE values of SVM Model are found to be low as comparative to SAM and MLH as shown in Table-2. The overall R^2 between observed and estimated values exceeds 0.95 (Figure-7) and the corresponding RMSE value has been determined as 0.03 (Table-2). These values indicate that the estimated land cover retrievals for Hyperion image bear a close relationship.

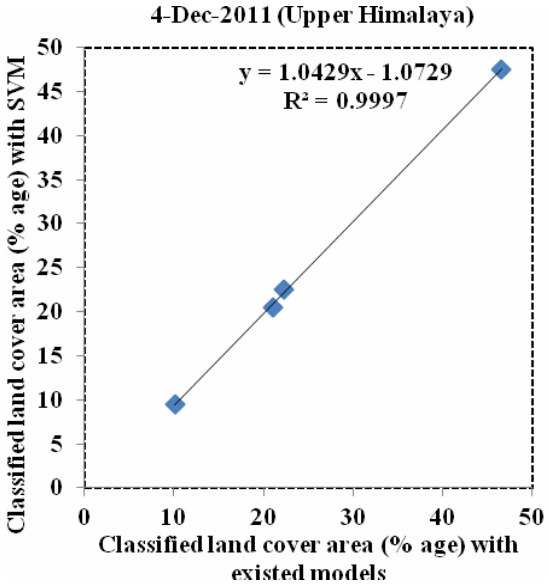

Figure-7. Comparative and correlation analysis between existed models and SVM with Hyperion (4-Dec-2011).

Table-1. Land covers classification in (% age) with various models.

Study area	Types of land cover	Land cover classification (area in % age) with				Error (area in % age)		
		Existed models (a)	SAM (b)	SVM (c)	MLH (d)	[a-b]	[a-c]	[a-d]
Middle Himalaya (13-Dec-2004)	Less contaminated snow/snow-ice mixed debris	68.63	54.00	68.82	36.78	14.63	0.19	31.85
	Non-snow area/soil/vegetation	31.37	42.96	31.18	63.22	11.59	0.19	31.85
	Unclassified	0	3.04	0	0	3.04	0	0
Upper Himalaya (4-Dec-2011)	No contamination/ pure snow	21.02	48.45	20.53	16.17	27.43	0.49	6.41
	Less contaminated snow/snow-ice mixed debris	46.60	16.35	47.51	52.12	30.25	0.91	5.52
	Debris	22.26	22.00	22.48	20.13	0.26	0.22	2.13
	Non-Snow area/soil/vegetation	10.12	13.04	9.48	11.58	2.92	0.64	1.46
	Unclassified	0	0.16	0	0	0.16	0	0
Average estimate error in area (% age)						11.29	0.33	9.90

Table-2. Root mean square error (RMSE).

Study area	Root mean square error (RMSE)			
	Imagery date	SAM	SVM	MLH
Middle Himalaya	13-Dec-2004	0.20	0.05	0.08
Upper Himalaya	04-Dec-2011	0.08	0.03	0.10

CONCLUSIONS AND DISCUSSIONS

Land covers classification is a fundamental component in ecological modeling and in any surface processes. The present paper discusses qualitative and quantitative analysis of various statistical methods on Hyperion satellite data and explore the potential of high resolution Hyperion data in land covers classification. Classification results with SAM and MLH methods are not very successful in Himalayan regions and produce poor

results. Mostly the shady areas in all ranges of Himalayas are unclassified with SAM technique. Extracted land surface parameters using SVM are quite similar in texture and areas on comparing with existed models. This is support SVM as an additional tool to retrieve land surface parameters with Hyperion. In few places, using SVM there is a small deviation which may be due to the selection of threshold values used for the conversion of indices to surface classes. It is important to note that the threshold values are likely to be scene dependent and empirical analysis may be necessary for each case. Further research is needed with imagery on a global basis to derive guidelines on which method performs best under which situation.

ACKNOWLEDGEMENTS

Author's sincere gratitude to USGS EROS data center, USA for providing Hyperion images. Thanks are also due to Sh. Aswagausha Ganju Director, Snow and Avalanche Study Establishment (SASE), Defence Research and Development Organization (DRDO), India for providing necessary facilities and for his kind motivation in the field of geomorphological research.

REFERENCES

Anderson G. P, Pukall B, Allred C. L, Jeong L. S, Hoke M, Chetwynd J. H, Adler-golden S. M, Berk A, Matthew M. W, Adler-Golden S. M, Berk A, Richtsmeier S.C, Levine R. Y, Bernstein L.S, Acharya P. K, Anderson G. P, Felde G.W, Hoke M.P, Ratkowski A, Burke H.H, Kaiser R.D and Miller D.P. 2000. Status of Atmospheric Correction Using a MODTRAN4-based Algorithm. SPIE Proceedings, Algorithms for Multispectral, Hyperspectral and Ultraspectral Imagery. 6: 199-207.

Assef M. M. 2004. Spatiotemporal dynamics of land surface parameters in the Red River of the North Basin, Physics and Chemistry of the Earth. 29: 79-810.

Bernstein L. S, Richtsmeier S. C, Acharya P. K and Matthew M. W. 1999. FLAASH and MODTRAN4: state-of-the-art atmospheric correction for hyperspectral data, IEEE Aerospace. Conference Proceeding. 4: 177-181.

Bindschadler R and Choi H. 2003. Characterizing and Correcting Hyperion Detectors Using Ice-Sheet Images. IEEE Transactions on Geoscience and Remote Sensing. 41(6): 1189-1193.

Cooley T, Anderson G.P, Felde G.W, Hoke M.L, Ratkowski A.J, Chetwynd J. H, Gardner J. A, Adler-golden S. M, Matthew M. W, Berk A, Bernstein L. S, Acharya P. K, Miller D and Lewis P. 2002. FLAASH a MODTRAN4-based atmospheric correction algorithm, its application and validation, IGARSS. 3: 1414-1418.

Datt B, McVicar T.R, Van Niel T.G, Jupp D.L.B and Pearlman J.S. 2003. Preprocessing EO- 1 Hyperion Hyperspectral Data to Support the Application of Agricultural Indexes. IEEE Transactions on Geoscience and Remote Sensing. 41(6): 1246-1259.

ENVI User's Guide. 2009. Version 4.7, Research Systems Inc., accessed on 15 July 2012.

Green A.A, Berman M, Switzer P and Craig M.D. 1988. A Transformation for Ordering Multispectral Data in Terms of Image Quality with Implications for Noise Removal. IEEE Transactions on Geoscience and Remote Sensing. 26(1): 65-74.

Hall D.K, Riggs G.A and Salomonson V.V. 1995. Development of methods for mapping global snow cover using moderate resolution imaging spectro-radiometer data. Remote Sensing Environment. 54: 127-140.

Haertel V. F and Shimabukuro Y.E. 2005. Spectral linear mixing model in Low spatial resolution image data. IEEE Transactions on Geoscience and Remote Sensing. 43(11): 2555-2562.

Hsu C.W, Chang C.C and Lin C.J. 2007. A practical guide to support vector classification. National Taiwan University. URL. http://ntu.csie.org/~cjlin/papers/guide/guide.pdf.

Jodha N. S. 2001. The Nepal middle mountains. www.unu.edu/unupress/unubooks/uu14re/uu14re0g.htm. Downloaded 26 August 2011.

Kaufman Y. J, Wald A. E, Remer L.A, Gao B.C, Li R.R and Flynn L. 1997. The MODIS 2.1-μm Channel-Correlation with Visible Reflectance for Use in Remote Sensing of Aerosol. IEEE Transactions on Geosciences and Remote Sensing. 35: 1286-1298.

Kruse F.A, Boardman J.W and Huntington J.F. 2003. Comparison of Airborne Hyperspectral Data and EO-1 Hyperion for Mineral Mapping. IEEE Transactions on Geoscience and Remote Sensing. 41(6): 1388-1400.

Kulkarni A.V, Singh S.K, Mathur P and Mishra V.D. 2006. Algorithm to monitor snow cover AWiFS data of RESOURCESAT-1 for the Himalayan region. International Journal of Remote Sensing. 27(12): 2449-2457.

Keshri A.K, Shukla A and Gupta R.P. 2009. ASTER ratio indices for supraglacial terrain mapping International journal of Remote Sensing. 30(2): 519-524.

Liang S. 2004. Quantitative remote sensing of land surfaces. Wiley series in remote sensing, Wiley-Interscience, Hoboken, NJ. 26: 534.

Metsamaki S, Vepsalainen J, Pullinainen J and Sucksdorff Y. 2002. Improved linear interpolation method for the

estimation of snow covered area from optical data, Remote Sensing of Environment. 82: 64-78.

Manjeet Singh, Mishra V.D, Jyoti Dhar Sharma and Anita Negi. 2012. Estimation of Snow Physical Parameters Using EO-1 Hyperion. IOSR Journal of Applied Physics. 1(6): 08-13.

Mishra V.D, Sharma J.K and Khanna R. 2010. Review of topographic analysis methods for the western Himalaya using AWiFS and MODIS satellite imagery. Annals of Glaciology. 51(54): 153-159.

Nolin A.W, Dozier J and Mertes L.A.K. 1993. Mapping alpine snow cover using a spectral mixture modelling technique. Annals of Glaciology. 17: 121-124.

Negi H. S, Singh S. K, Kulkarni A. V and Semwal B. S. 2010. Field-based spectral reflectance measurements of seasonal snow cover in the Indian Himalaya. International Journal of Remote Sensing. 31: 9, 2393-2417.

Pearlman J.S, Barry P.S, Segal C.C, Shepanski J, Beiso D and Carman S.L. 2003. Hyperion, a Space-Based Imaging Spectrometer. IEEE Transactions on Geoscience and Remote Sensing. 41(6): 1160-1173.

Rosenthal W and Dozier J. 1996. Automated mapping of montane snow covers at subpixel resolution from the Landsat Thematic Mapper, Water resources Research. 322: 115-130.

Richards J.A. 1999. Remote Sensing Digital Image Analysis, Springer-Verlag, Berlin. p. 240.

Rogan J and Chen D. 2004. Remote Sensing Technology for mapping and monitoring land cover and land-use change. Process in Planning. 61: 301-325.

Simpson J.J, Stitt J.R and Sienko M. 1998. Improved estimates of the areal extent of snow cover from AVHRR data. Journal of Hydrology. 204: 1089-1104.

Salomonson V.V and Appel I. 2004. Estimating fractional snow-cover from MODIS using the normalized difference snow index. Remote Sensing of the Environment. 89: 351-360.

USGS. 2003. EO-1 User Guide version 2.3, downloaded 2 December 2012, from, eo1.usgs.gov/documents/EO1userguidev2pt320030715UC.pdf.

Vikhamar D and Solberg R. 2002. Subpixel mapping of snow cover in forests by optical remote sensing. Remote Sensing of Environment. 84: 69-82.

Xiao X, Z. Shen and X Qin. 2001. Assessing the potential of VEGETATION sensor data for mapping snow and ice cover: A normalized difference snow and ice index. International Journal of Remote Sensing. 22:2479-2487.